

Optical and electrical properties of Al-rich AlGaN alloys

J. Li, K. B. Nam, J. Y. Lin, and H. X. Jiang

Citation: *Applied Physics Letters* **79**, 3245 (2001); doi: 10.1063/1.1418255

View online: <http://dx.doi.org/10.1063/1.1418255>

View Table of Contents: <http://scitation.aip.org/content/aip/journal/apl/79/20?ver=pdfcov>

Published by the *AIP Publishing*

Articles you may be interested in

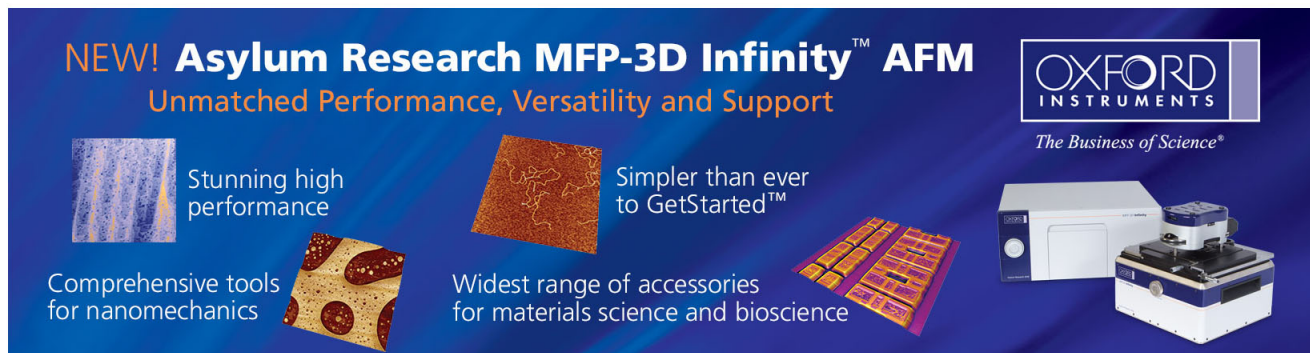
[Optical properties and carrier dynamics of two-dimensional electrons in Al Ga N Ga N single heterostructures](#)
Appl. Phys. Lett. **87**, 041909 (2005); 10.1063/1.2000334

[Growth and optical studies of two-dimensional electron gas of Al-rich AlGaN/GaN heterostructures](#)
Appl. Phys. Lett. **81**, 1809 (2002); 10.1063/1.1504881

[Excitonic luminescence linewidths in AlGaN alloys with high aluminum concentrations](#)
Appl. Phys. Lett. **80**, 2907 (2002); 10.1063/1.1471932

[Optical and electrical properties of Mg-doped p-type Al_xGa_{1-x}N](#)
Appl. Phys. Lett. **80**, 1210 (2002); 10.1063/1.1450038

[Linewidths of excitonic luminescence transitions in AlGaN alloys](#)
Appl. Phys. Lett. **78**, 1829 (2001); 10.1063/1.1357212

The advertisement features a dark blue background with white and orange text. At the top left, it reads 'NEW! Asylum Research MFP-3D Infinity™ AFM' in large white letters, followed by 'Unmatched Performance, Versatility and Support' in orange. To the right is the Oxford Instruments logo, which includes the text 'OXFORD INSTRUMENTS' and the tagline 'The Business of Science®'. Below the main text are four images: a textured surface, a circular pattern, a grid of small squares, and the AFM instrument itself. Each image is accompanied by a short text description: 'Stunning high performance', 'Simpler than ever to GetStarted™', 'Comprehensive tools for nanomechanics', and 'Widest range of accessories for materials science and bioscience'.

Optical and electrical properties of Al-rich AlGa_xN alloys

J. Li, K. B. Nam, J. Y. Lin, and H. X. Jiang^{a)}

Department of Physics, Kansas State University, Manhattan, Kansas 66506-2601

(Received 26 June 2001; accepted for publication 4 September 2001)

Al_xGa_{1-x}N alloys with x up to 0.7 were grown by metalorganic chemical vapor deposition and their optical properties were investigated by deep UV time-resolved photoluminescence (PL) spectroscopy. Our results revealed that both the activation energy of the PL emission intensity and the PL decay lifetime exhibit sharp increases at x of around 0.4. The results can be understood in terms of the sharp increase of the impurity binding energy or the carrier/exciton localization energy around $x=0.4$. A three orders of magnitude increase in resistivity of undoped AlGa_xN alloys at x of around 0.4 was also observed, which further corroborated the optical results. © 2001 American Institute of Physics. [DOI: 10.1063/1.1418255]

With recent rapid progress in III-nitride based devices, materials growth and fundamental understanding of the optical and electrical properties of Al-rich AlGa_xN alloys have become increasingly important. Al-rich Al_xGa_{1-x}N alloys are both difficult to grow and to characterize due to having much wider energy band gaps than GaN. However, Al-rich AlGa_xN alloys are indispensable in deep UV light emitters as well as in high performance electronic devices.^{1,2} GaN and AlN form alloys with direct band gaps, whose band gaps range from 3.4 to 6.2 eV, giving an energy gap difference ΔE_g of 2.8 eV. This is much larger than the typical value of a few tenths of eV in II-VI semiconductor alloys, in which a strong localization effect is known to exist.

In this letter, we report the growth and optical and electrical properties of Al_xGa_{1-x}N alloys for x up to 0.7. Our results have revealed that the photoluminescence (PL) emission intensity decreases with an increase of the Al content. On the other hand, the activation energy of the impurity level or the carrier/exciton location energy in Al_xGa_{1-x}N alloys was found to increase sharply at x of around 0.4. These results provide further information regarding both n - and p -type conductivity of Al_xGa_{1-x}N with $x > 0.4$.

Al_xGa_{1-x}N epilayers ($x < 0.7$) 1 μm thick were grown by metalorganic chemical vapor deposition (MOCVD) on sapphire (0001) substrates with 25 nm low temperature AlN nucleation layers. The growth temperature and pressure were 1060 °C and 80 Torr, respectively. Trimethylgallium (TMG) and trimethylaluminum (TMAI) were used as the metalorganic sources. In order to measure the time-resolved PL of Al-rich AlGa_xN alloys, a deep UV (195 nm) laser system was specifically designed to generate femtosecond (100 fs) tunable laser pulses with 10 mW average power and 76 MHz repetition rate. More detailed information about the deep UV laser system can be found in Ref. 3. A single photon counting detection system together with a microchannel plate (MCP) photomultiplier tube (PMT) and a streak camera with a detection capability ranging from 185 to 800 nm were used to record continuous wave (cw) and time-resolved PL spectra. The Al composition of the AlGa_xN alloys was determined

by the flow rates of TMG and TMAI as well as by an energy dispersive x-ray chemical microanalyzer (model 4060 Oxford) and from the PL peak positions by assuming the energy band gap E_g of AlGa_xN follows

$$E_g(x) = (1-x)E_g(\text{GaN}) + xE_g(\text{AlN}) - bx(1-x), \quad (1)$$

with the bowing parameter $b = 0.98 \text{ eV}$.⁴ Values of 3.42 and 6.20 eV were used for the room temperature energy band gaps of GaN and AlN, respectively. The Al contents for selective samples were also determined by x-ray diffraction and secondary ion mass spectroscopy (performed by Charles Evans & Assoc.) measurements. All these methods provide consistent Al compositions with accuracy within ~ 0.02 .

Low-temperature (10 K) cw PL spectra of Al_xGa_{1-x}N alloys with $x = 0.3, 0.5, \text{ and } 0.7$ are presented in Fig. 1. The PL peak position, E_p , the full width at half maximum (FWHM), as well as integrated intensity, S , are also indicated. Besides the shift of the peak position towards shorter wavelength with increasing Al content, one can also notice a considerable decrease in the PL intensity and an increase in the FWHM, which is caused by alloy broadening. The solid lines are the least-squares fits of data with two peaks of Gaussian distributions. With longitudinal optical (LO) pho-

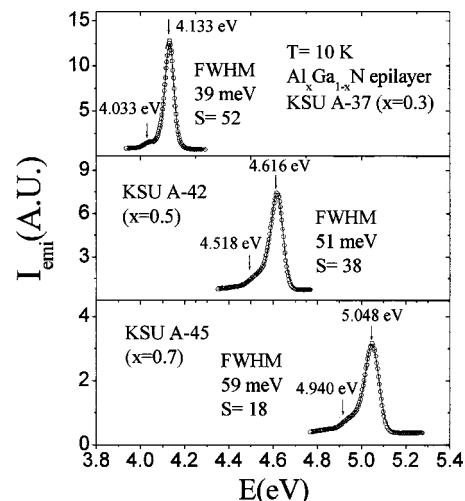


FIG. 1. Low-temperature (10 K) cw PL spectra of Al_xGa_{1-x}N alloys with $x = 0.3, 0.5, \text{ and } 0.7$.

^{a)}Electronic mail: jiang@phys.ksu.edu

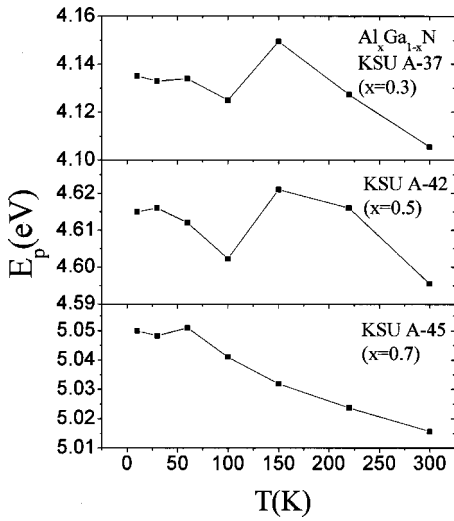


FIG. 2. Temperature variations of the main PL emission peak positions, E_p , of $\text{Al}_x\text{Ga}_{1-x}\text{N}$ alloys with $x=0.3, 0.5,$ and 0.7 .

non energies around 112 and 92 meV for AlN and GaN, respectively,⁵ the low energy shoulders in Fig. 1 are assigned to LO phonon replicas of the main emission peak.

Figure 2 shows temperature variations of the main emission peak positions (E_p) of $\text{Al}_x\text{Ga}_{1-x}\text{N}$ alloys with $x=0.3, 0.5,$ and 0.7 , where values of E_p were determined by fitting the PL spectra near the emission peaks by Gaussian functions. The E_p versus temperature plots shown in Fig. 2 for $x=0.3$ and 0.5 clearly depict the S-shape behavior, similar to in the case for AlGaIn alloys with low Al content ($x < 0.35$).^{6,7} The S-shape behavior has been explained in terms of the effects of localized states induced by alloy fluctuations in AlGaIn alloys. The systematic behavior exhibited by the data of Fig. 2 for $x=0.3$ and 0.5 may be understood in terms of the impurity bound or localized exciton transition in the tail states due to alloy fluctuation. Similar behavior has been reported previously for the temperature-dependent PL emission energy shift in InGaIn/GaN multiple quantum wells⁸ and in pseudomorphic AlGaIn/GaN heterostructures.⁹ However, the E_p versus temperature behavior for the $x=0.7$ AlGaIn

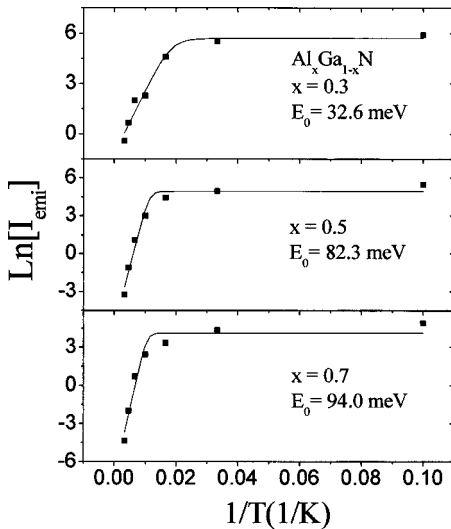


FIG. 3. Arrhenius plots of the PL intensity for AlGaIn alloys with $x=0.3, 0.5,$ and 0.7 . The solid lines are the least-squares fit of data with Eq. (2). The fitted activation energy, E_0 , is also indicated.

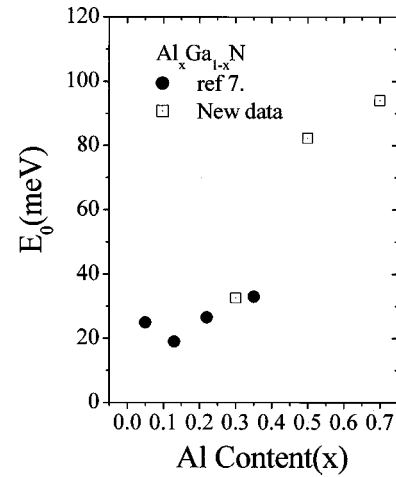


FIG. 4. Activation energy E_0 as a function of Al composition x . A dramatic increase of E_0 is evident at $x \sim 0.4$.

alloy is quite different than that of $x=0.3$ and 0.5 . For $x=0.7$, the fluctuation is so large that the S shape is less pronounced or it has disappeared.

Figure 3 shows Arrhenius plots of the PL emission intensity of $\text{Al}_x\text{Ga}_{1-x}\text{N}$ alloys with $x=0.3, 0.5,$ and 0.7 . The solid lines are the least-squares fit of data with

$$I_{\text{emi}}(T) = I_0 / [1 + C \exp(-E_0/kT)], \quad (2)$$

where E_0 is the activation energy of the PL emission intensity. The fitted activation energy E_0 is indicated in Fig. 3. Figure 4 shows a plot of the Al composition (x) dependence of the activation energy, E_0 , obtained for the set of three samples together with AlGaIn alloys of low Al content.⁷ The most intriguing result is that E_0 has a sharp increase at $x \sim 0.4$. For $x > 0.5$, E_0 is as large as 90 meV, much larger than the thermal energy at room temperature (25 meV).

There are many important consequences for large E_0 for x greater than 0.4. Larger E_0 implies larger impurity binding energies or carrier/exciton localization energies, which will make the conductivity of these materials very low, a fact that is well known for Al-rich AlGaIn alloys.¹⁰ It has been suggested that the binding energies of impurities in $\text{Al}_x\text{Ga}_{1-x}\text{N}$ increase with x , and cause low conductivities for undoped Al-rich AlGaIn alloys.¹⁰ We have measured the conductivity of a set of undoped AlGaIn alloys with x between 0.3 and 0.5 and the results are summarized in Table I. As shown in Table I, the resistivity increases by about three orders of magnitude when the Al content is increased from 0.3 to 0.4. It becomes a highly resistive material at x of around 0.5 for undoped $\text{Al}_x\text{Ga}_{1-x}\text{N}$ alloys. The results shown in Table I further corroborate the optical data presented in Fig. 4.

TABLE I. Resistivity of undoped $\text{Al}_x\text{Ga}_{1-x}\text{N}$ alloys with x varying from 0.3 to 0.5.

Al content, x	Resistivity ρ (Ω cm)
0.3	0.18
0.35	2.1
0.4	190
0.45	374
0.5	$> 10^5$

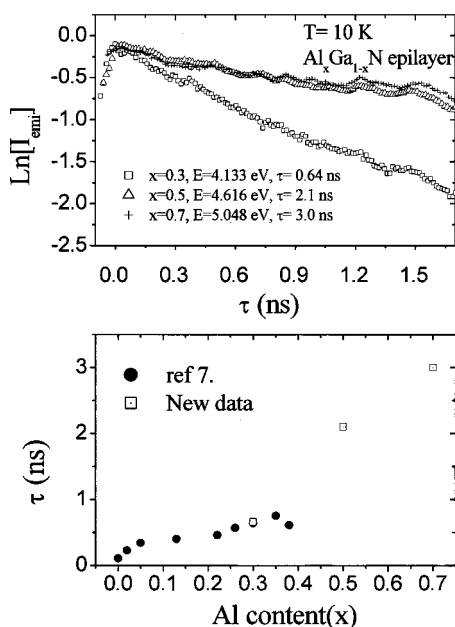


FIG. 5. Temporal responses for the PL emissions from Al_xGa_{1-x}N alloys with $x=0.3$, 0.5 , and 0.7 measured at 10 K and their emission peak positions. (b) The Al content dependence of the measured decay lifetime ($T=10\text{ K}$) of Al_xGa_{1-x}N alloys. A similar trend for results shown in (a) and in Fig. 4 is evident.

Time-resolved PL spectra were measured at 10 K . Figure 5(a) shows the temporal responses of the PL emissions from AlGa_N alloys (with $x=0.3$, 0.5 , and 0.7) measured at their respective spectral peak positions. It clearly shows an increase in the decay lifetime with increasing Al content. Figure 5(b) shows a plot of the decay lifetimes of these three samples together with those of low Al content AlGa_N alloys obtained previously.⁷ Quite convincingly, the decay lifetime shows exactly the same trend as that of the activation energy

of the PL emission intensity shown in Fig. 4. The PL decay lifetime is expected to increase with the impurity binding energy as well as with the carrier/exciton localization energy.^{7,11}

In summary, we have investigated the optical and electrical properties of Al_xGa_{1-x}N alloys for x up to 0.7 . Our results strongly suggest either a deepening of the impurity level or a sharp increase of the localization energy in high Al content AlGa_N alloys is responsible for the various behaviors reported here. These include sharp increases of the PL emission intensity activation energy, of the PL decay lifetime, and of the resistivity for undoped Al_xGa_{1-x}N alloys at x of around 0.4 .

This research was supported by grants from DOE (No. 96ER45604/A000), NSF (Nos. DMR-9902431 and INT-9729582), ONR, ARO, and BMDO.

¹S. Nakamura and G. Fasol, *The Blue Laser Diode* (Springer, New York, 1997).

²K. B. Nam, J. Li, H. Kim, J. Y. Lin, and H. X. Jiang, *Appl. Phys. Lett.* **78**, 3690 (2001).

³<http://www.phys.ksu.edu/area/GaNgroup>

⁴M. R. H. Khan, Y. Koide, H. Itoh, N. Sawaki, and I. Akasaki, *Solid State Commun.* **60**, 509 (1986).

⁵*Semiconductors—Basic Data*, 2nd revised ed., edited by O. Madelung (Springer, Berlin, 1996).

⁶Y. H. Cho, G. H. Gainer, J. B. Lam, J. J. Song, W. Yang, and W. Jhe, *Phys. Rev. B* **61**, 7203 (2000).

⁷H. S. Kim, R. A. Mair, J. Li, J. Y. Lin, and H. X. Jiang, *Appl. Phys. Lett.* **76**, 1252 (2000).

⁸Y.-H. Cho, G. H. Gainer, A. J. Fischer, J. J. Song, S. Keller, U. K. Mishra, and S. P. DenBaars, *Appl. Phys. Lett.* **73**, 1370 (1998).

⁹G. Steude, B. K. Meyer, A. Göldner, A. Hoffmann, F. Bertram, J. Christen, H. Amano, and I. Akasaki, *Appl. Phys. Lett.* **74**, 2456 (1999).

¹⁰M. D. Bremser, *Gallium Nitride and Related Semiconductors*, edited by J. H. Edgar, S. Strite, I. Akasaki, H. Amano, and C. Wetzel (Institute of Electrical Engineers, London, 1999), p. 147.

¹¹G. D. Chen, M. Smith, J. Y. Lin, H. X. Jiang, M. Asif Khan, and C. J. Sun, *Appl. Phys. Lett.* **67**, 1653 (1995).